PROCEEDINGS OF SCIENCE

Cosmic-Ray Transport between the Knee and the Ankle with CRPropa

Lukas Merten[*a], **Julia Tjus**[a], **Chad Bustard**[b], **and Ellen G. Zweibel**[bc]

[a] *Theoretische Physik IV, Ruhr University Bochum, Universitätsstrasse 150, 44801 Bochum - Germany*

[b] *Department of Physics, University of Wisconsin-Madison, 1150 University Avenue, Madison, WI 5370*

[c] *Department of Astronomy, University of Wisconsin-Madison, 2535 Sterling Hall, 475 N. Charter Street, Madison, WI 537*

E-mail: lukas.merten@rub.de, julia.tjus@rub.de, bustard@wisc.edu, zweibel@astro.wisc.edu

An appropriate numerical modeling of cosmic-ray transport is a major challenge in modern astroparticle physics. Multi-messenger observations of cosmic rays and their neutral secondary particles like neutrinos and gamma-rays must relate to source models. This requires a detailed description of the propagation and interaction of all particles.

Especially in the region between the cosmic-ray knee and ankle, where the transition between Galactic and extra-galactic sources is expected, the modeling of cosmic-ray transport is complicated. Classical simulation frameworks are usually dedicated to lower or to the very highest energies. These software tools use grid-based methods to solve the transport equation (low energies) or propagate single particles solving the equation of motion (highest energies). Both techniques having different problems in the transition region.

In this work an innovative technique—based on stochastic differential equations—to solve the transport equation is explained. The ansatz of propagating independent phase-space elements (or pseudo-particles) allows for easy parallelization which makes it attractive for modern large-scale computing architectures. It combines the numerical framework of the single particle propagation with the advantage of ensemble averaged description of the transport equation. Making it an ideal tool to describe the transition between Galactic and extra-galactic cosmic-rays.

This approach is implemented in the latest version of the publicly available propagation software CRPropa and already applied to various problems. The influence of different source distributions on the global Galactic cosmic-ray density and the transport of cosmic-rays from the Galactic Wind Termination shock are discussed as an example.

36th International Cosmic Ray Conference -ICRC2019-
July 24th - August 1st, 2019
Madison, WI, U.S.A.

*Speaker.

PoS(ICRC2019)350

1. Transport of highly relativistic cosmic rays

In general, the description of the propagation of charged particles in magnetic fields, is a non-linear highly coupled problem. Cosmic rays are deflected by magnetic fields and the magnetic fields are altered by, e.g., plasma instabilities caused by the motion of the cosmic rays. A realistic solution taking all these effects into account is not yet possible on long time scales. So called Particle-In-Cell (PIC) simulations are aiming at a complete description of the transport process but are up to now limited to small spatial volumes and short time scales, compared with the lifetime of cosmic rays in the Galaxy.

When only cosmic rays with energies above $E_{\mathrm{min}} = 10$ TeV are considered, the energy density in cosmic rays is much smaller than in the magnetic field of the Milky way, $w_{\mathrm{CR}} \ll \langle B^2 \rangle / (8\pi)$. In this case the influence of cosmic rays on the magnetic field structure can be neglected just by energetic arguments. The system of cosmic rays and magnetic fields decouples. Assuming an isotropic cosmic-ray distribution $n(\vec{r}, p, t)$, where the particle density does not depend on the direction of the momentum vector, the transport equation, describing the time evolution of the cosmic-ray ensemble yields:

$$\frac{\partial n}{\partial t} = \nabla \cdot (\hat{\kappa} \nabla n) - \vec{u} \cdot \nabla n + \frac{\partial}{\partial p} \left[p^2 \kappa_{pp} \frac{\partial}{\partial p} \left(\frac{n}{p^2} \right) \right] + \frac{p}{3} \nabla \cdot \vec{u} \frac{\partial}{\partial p} n + S(\vec{r}, p, t) \quad . \tag{1.1}$$

Here, $\hat{\kappa}$ is the spatial diffusion tensor, $\vec{u}$ is the advection speed, κ_{pp} is the momentum diffusion scalar, and all sources and sinks are summed up into the term S. Modeling, e.g., the primary-to-secondary-ratio makes it necessary to solve one transport equation (equ. (1.1)) per elemental group and couple these equations via the source/loss term S.

Conventionally, the transport equation is discretized on a grid and solved numerically with software frameworks like GalProp [20], DRAGON [4, 6], or PICARD [12, 13]. Mathematically equivalent is, however, also a description based on stochastic differential equations:

$$\mathrm{d}\vec{x} = \vec{u}\,\mathrm{d}t + \hat{D}\,\mathrm{d}\vec{w} \quad , \tag{1.2}$$

$$\mathrm{d}p = -\frac{p}{3} \nabla \cdot \vec{u}\,\mathrm{d}t + D_{pp}\,\mathrm{d}w_p \quad . \tag{1.3}$$

Here, the deterministic motion is described by the advection field $\vec{u}$ similar to equ. (1.1). The diffusive motion is described by the second summand, where $\mathrm{d}\vec{w}$ and $\mathrm{d}w_p$ are three- and one-dimensional Wiener-processes, respectively. The diffusion coefficients are connected to the real diffusion tensor via $\kappa_{ij} + \kappa_{ji} = D_{ik} D^*_{jk}$. For an overview on the mathematical framework of stochastic differential equations (SDEs) and their equivalence to Fokker-Planck partial differential equations the reader is referred to, e.g., the textbook [9].

One of the biggest advantages of the SDE approach is the independence of any spatial grid. Furthermore, as information on every phase space trajectory is available, a post-processing or reweighting of the simulation results is possible. That method, also known from single particle propagation, can drastically reduce the number of models, which have to be simulated.

2. Numerical solution

The latest version of the publicly available simulation software CRPropa [1] includes an SDE solver to treat the transport equation. In this work, only a short summary of the implementation is given and the interested reader is referred to the original publications in [15, 17] for more information. A unique feature of this specific implementation is the solution of the stochastic part of the SDE in the local frame of the magnetic field. The trihedron of the tangential, normal, and binormal vector of the field line, $\{\vec{e}_\mathrm{t}, \vec{e}_\mathrm{n}, \vec{e}_\mathrm{b}\}$, form an orthonormal basis. In this frame the diffusion tensor becomes diagonal $\hat{\kappa} = \mathrm{diag}(\kappa_\parallel, \kappa_\perp, \kappa_\perp)$ (see e.g. [19]). Neglecting momentum diffusion[1] ($\kappa_{pp} = 0$), the Ito-SDEs (equs. (1.2) (1.3)) can numerically be solved using the Euler-Maruyama scheme yielding:

$$\begin{aligned} \vec{x}_{n+1} - \vec{x}_n = & \underbrace{\vec{u}\,\Delta t}_{\text{Advection}} + \underbrace{\hat{D}\,\Delta \vec{w}_r}_{\text{Diffusion}} \\ & = (u_x \vec{e}_x + u_y \vec{e}_y + u_z \vec{e}_z) \cdot h \\ & + \left(\sqrt{2\kappa_\parallel}\,\eta_\parallel\,\vec{e}_\mathrm{t} + \sqrt{2\kappa_{\perp,1}}\,\eta_{\perp,1}\,\vec{e}_\mathrm{n} + \sqrt{2\kappa_{\perp,2}}\,\eta_{\perp,2}\,\vec{e}_\mathrm{b} \right) \cdot \sqrt{h} \quad , \end{aligned} \tag{2.1}$$

$$p_{n+1} - p_n = -p/3\,(\nabla \cdot \vec{u}) \cdot h \quad . \tag{2.2}$$

Here, the integration time step is given by h and η_i are Gaussian pseudo-random variables with zero mean and unit variance.

The remaining problem is the on-the-fly calculation of the local trihedron. In CRPropa's module `DiffusionSDE` an adaptive Cash-Karp algorithm is used to approximate the tangential direction $\vec{e}_t$. The other two directions are randomly drawn in the perpendicular plane because the normal and binormal direction can be assumed to be degenerated for Galactic magnetic field structures. Solving the SDE in the laboratory frame as, e.g., in [14, 18] makes a re-implementation of the space-dependent diffusion tensor necessary, whenever a different magnetic field should be used. Furthermore, the calculation of the tensor $\hat{D}$ is more complicated in the laboratory frame as $\hat{\kappa}$ is not diagonal in general. The CRPropa implementation of the SDE solver, based on the local trihedron, allows for a more flexible exchange of the background magnetic field model as the diffusion tensor is automatically adapted to the field.

As mentioned above a re-weighting of recorded data can be very valuable to reduce the number of simulations needed for the desired parameter scan. The re-weighting can be as simple as changing the index of the energy spectrum of the source or creating a model with finite source duration from data that was obtained from simulations of a single burst in time $S \propto \delta(t - t_0)$ (see e.g. [16] for a detailed description).

3. Cosmic Rays from the Galactic Wind Termination Shock

The sources of cosmic-rays between the knee and the ankle are still unknown. Beside the possibility of an extended Galactic component connected to, e.g., Wolf-Rayet stars [21],

[1] This is not a principle issue but momentum diffusion is not yet implemented in CRPropa.

the Galactic wind termination shock (GWTS) is a long discussed source candidate in this shin region, e.g., [11].

Assuming that the GWTS is able to accelerate cosmic rays to energies above $E \geq 10^{15}$ eV [3], it is not clear without dedicated simulations if these cosmic rays can propagate back into the Galaxy or are lost to the intergalactic medium. In the following, the main points of such a study of the propagation of GWTS cosmic rays are recapped from [17].

It is assumed that cosmic rays are accelerated at the GWTS at $r_{\text{shock}} = 250$ kpc with a source luminosity of $L_{\text{GWTS}} = 10^{40}\,\text{erg}\,\text{s}^{-1}$ deposited in a power law spectrum with $\Phi \propto E^{-2}$ and $E = (1 - 10^7)$ GeV; only particles above $E_{\text{min}} = 10^6$ GeV are eventually simulated. Furthermore, the source is modeled as being active for $\Delta T = 100$ Myr which is at the upper limit for a GWTS in the Milky Way [2]. The cosmic rays propagate according to an anisotropic diffusion tensor with normalization $\kappa = 5 \times 10^{28} \cdot (R/4\,\text{GV})^{\delta}$ and diffusion ratio $\epsilon = \kappa_{\perp}/\kappa_{\parallel}$ in a magnetic background field forming an Archimedean spiral:

$$\frac{\vec{B}}{B_0} = \underbrace{\left[1 - 2S\left(\theta - \frac{\pi}{2}\right)\right]}_{\text{change direction at z=0}} \left(\frac{r_{\text{ref}}^2}{r^2}\vec{e}_r - \frac{\Omega r_{\text{ref}}^2 \sin(\theta)}{r u_0}\vec{e}_{\phi}\right) \quad , \tag{3.1}$$

where, $\Omega r_{\text{ref}} \sin(\theta) = 200\,\text{km}\,\text{s}^{-1}$ is the rotational velocity at the reference level $r_{\text{ref}} = 10$ kpc and $u_0 = 600\,\text{km}\,\text{s}^{-1}$ is the constant wind velocity. The magnetic field strength has no influence on the simulation as only the direction is used for the diffusion.

The wind field is given by:

$$\vec{u}(\vec{r}) = u_0 \cdot \left[1 + \frac{\left(\frac{r_0}{2r}\right)^2 - 1}{1 + \exp\left(-\frac{r - r_0}{\lambda}\right)}\right] \cdot \vec{e}_r + u_{\phi} \cdot \frac{r_{\text{ref}}}{r} \cdot \vec{e}_{\phi} \quad . \tag{3.2}$$

Here, $\lambda = 50$ pc is a parameter controlling the width of the shock and therefore also the minimum of the wind divergence, which is connected to the heating rate. It was fixed for all simulations shown here.

Figure 1 shows the magnetic and wind field pattern in the Galactic plane. The shock is clearly visible in the wind speed.

3.1 Results

Figure 2 shows as an example the expected energy spectra at the observer sphere outside of the Galaxy ($r_{\text{obs}} = 10$ kpc). The time evolution of the spectrum is color coded, where the observation time is measured from the beginning of the source duration. Independent of the diffusion ratio ϵ the observed spectrum does get broader with time. In the case of perpendicular diffusion ($\epsilon = 0.1$) the initial spectrum is less altered than for pure parallel diffusion (right panel). The significant adiabatic re-acceleration of cosmic rays observed in the parallel spectra, especially for later times, has to be caused by a long duration in the shock region. The low escape probability from the shock can easily be explained by the field line geometry in the source region, which is almost parallel to the shock plane at least at the Galactic equator. As cosmic rays cannot leave their initial field line for pure parallel transport this can explain the large energy gain.

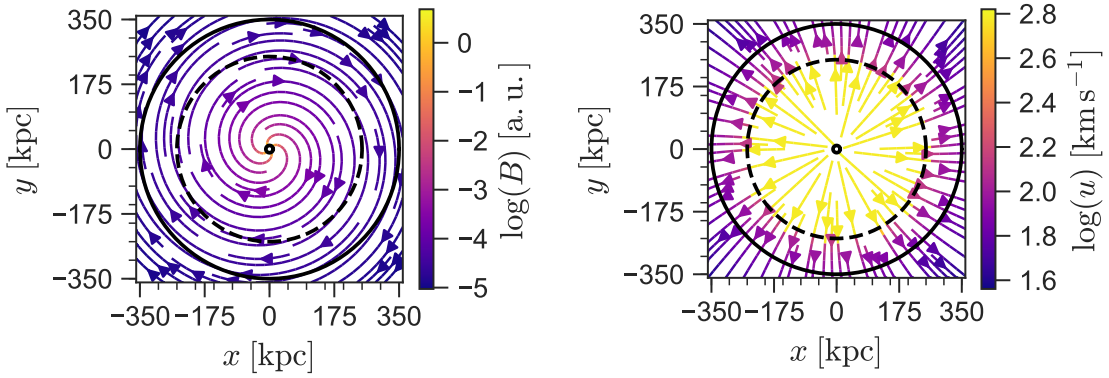

Figure 1: Face on view of the magnetic field and the Galactic wind in the Galactic plane. The inner solid circle is the oberver sphere and the outer solid circle is the free escape boundary. The shock position is marked by the dashed circle.

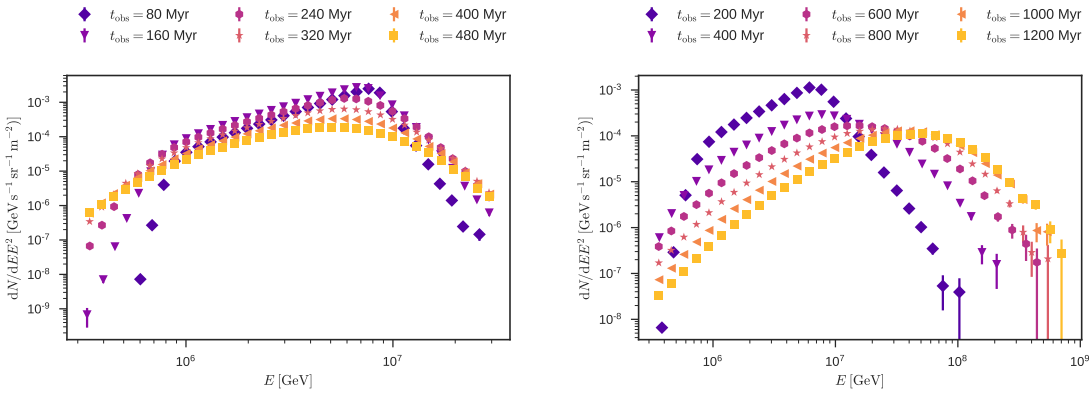

Figure 2: Energy spectrum at the spherical observer sphere $r_{obs} = 10$ kpc. Left including perpendicular diffusion $\epsilon = 0.1$ and right pure parallel diffusion.

Figure 3 shows the arrival direction pattern averaged over the symmetric right ascension coordinate. For pure parallel diffusion (dashed lines) a prominent double bump structure, which shifts with time from the poles to the equator, is visible. This structure is caused by different magnetic field line lengths depending on the Galactic latitude; an equatorial field line is five times longer than a polar one. Including perpendicular diffusion reduces the level of anisotropy. However, the level of expected anisotropy is still challenging the observed isotropy limits.

Figure 4 shows the relative energy change caused by the Galactic wind (left panel) and the expected cosmic-ray luminosity compared with different model expectations (right panel). It is clearly visible that most of the cosmic rays will lose energy during the propagation only in the case of pure parallel diffusion with a Kraichnan diffusion index of $\delta = 0.5$ the ensemble as a whole will gain energy.

To compare the resulting cosmic-ray luminosity with expectations the analytic cosmic-

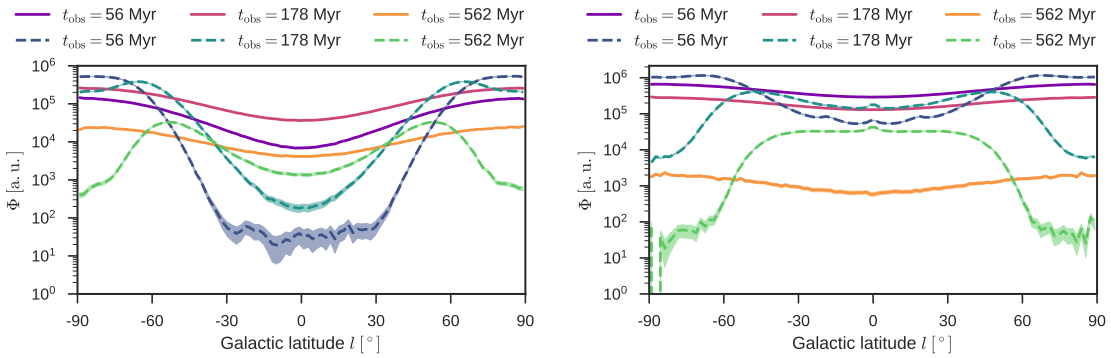

Figure 3: Right ascension averaged arrival direction of cosmic rays at $r_{obs} = 10$ kpc. Including perpendicular diffusion (solid lines) leads to a much smoother arrival pattern. Left panel shows a diffusion index of $\delta = 0.5$ and right panel of $\delta = 0.6$, respectively.

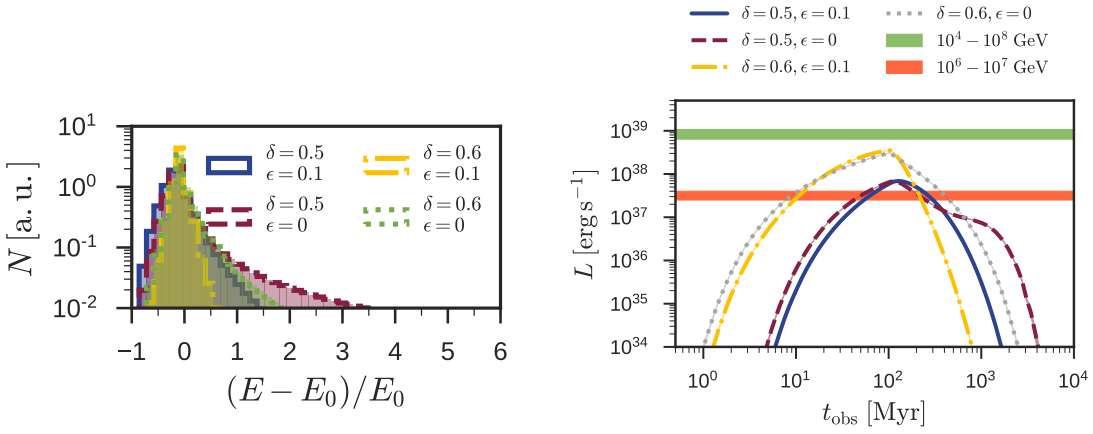

Figure 4: Left panel shows the relative energy change caused by adiabatic compression or expansion for different diffusion models. Right panel shows the expected cosmic-ray luminosity compared to the total Galactic cosmic-ray luminosity given in different phenomenological models [5, 7, 8, 10, 22] for two integration boundaries.

ray fluxes given in different phenomenological models [5, 7, 8, 10, 22] are integrated over the energy:

$$L_{CR}(E_{min}, E_{max}) = \frac{4\pi V \cdot \int_{E_{min}}^{E_{max}} \Phi \, E \, dE}{c_0 \, \tau_{esc}} \quad . \tag{3.3}$$

Here, an escape time of $\tau = 10$ Myr and a volume filled by cosmic rays $V = 200\,\text{kpc}^3$ have been assumed. Two different integration limits are shown, one corresponding to the injection energy range (orange) and one to the final energy range (green). Most models cannot account for the complete observed cosmic-flux in the transition region. However, the GWTS can be a significant source of cosmic rays between the knee and the ankle.

4. Summary and Outlook

In this work the SDE solver implemented in CRPropa was described and first applications have been discussed. The module `DiffusionSDE` is able to handle anisotropic diffusion ($\kappa_\parallel \neq \kappa_\perp$) in arbitrary coherent magnetic background fields, defined by analytic functions or on a spatial grid. The modular structure of the CRPropa framework based on individual modules makes it easy to extend the software in the future to, e.g., include momentum diffusion or allow for spatially varying eigenvalues of the diffusion tensor.

The GWTS was examined as a possible source candidate for cosmic rays in the shin region. It was shown that indeed a significant amount of cosmic rays can diffuse back into the Galaxy. During their propagation most of the particles are adiabatically cooled, however, some cosmic rays are re-accelerated by compression in the shock region up to a factor of 10 and more. The estimated arrival pattern caused by the Archimedean spiral excludes a pure parallel diffusion for anisotropy reasons. However, in the case of perpendicular diffusion the arrival direction is less problematic.

The logical next step for a GWTS simulation is to propagate the cosmic rays further into the Galaxy. In doing so, the influence of the additional Galactic propagation on the arrival direction can be analyzed.

In the future, the newly developed tools can be used to analyze the transition between Galactic and extra-galactic sources further. The opportunities of the SDE approach was demonstrated already with the application to the GWTS.

When the implementation of hadron-hadron interaction is finished, CRPropa can be used to model full scale simulation to, e.g., examine the Galactic gamma-ray gradient problem. In addition, comparing simulation results with observed boron-to-carbon ratios and other tracers will help to understand the diffusion tensor better.

Acknowledgments

The software development was only possible by the help of the CRPropa development team, especially by G. Sigl, T. Winchen, and A. Dundovic. For further valuable discussions the authors thank B. Eichmann and H. Fichtner.

References

[1] R. Alves Batista et al. In: *J. Cosm. and Astr. Phys.* 5, 038 (May 2016).

[2] C. Bustard et al. In: *The Astroph. J.* 819, 29 (2016).

[3] C. Bustard et al. In: *The Astroph. J.* 835, 72 (2017).

[4] C. Evoli et al. In: *J. Cosm. and Astr. Phys.* 10.10 (Oct. 2008).

[5] A. Fedynitch et al. In: *Phys. Rev. D* 86, 114024 (2012).

[6] D. Gaggero et al. In: *Phys. Rev. Lett.* 111.2 (July 2013).

[7] T. K. Gaisser. In: *Astropart. Phys.* 35 (2012).

[8] T. K. Gaisser and M. Honda. In: *Annual Review of Nuclear and Particle Science* 52 (2002).

[9] C. Gardiner. Springer Series in Synergetics. Springer Berlin Heidelberg, 2009. ISBN: 9783540707127.

[10] J. R. Hörandel. In: *Astropart. Phys.* 21 (2004).

[11] J. R. Jokipii and G. E. Morfill. In: *The Astroph. J.* 312 (1987).

[12] R. Kissmann. In: *Astropart. Phys.* 55 (Mar. 2014).

[13] R. Kissmann et al. In: *Astropart. Phys.* 70 (Oct. 2015).

[14] A. Kopp et al. In: *Computer Physics Communications* 183.3 (Mar. 2012).

[15] L. Merten et al. In: *J. Cosm. and Astr. Phys.* 6, 046 (2017).

[16] L. Merten. PhD thesis. Ruhr University Bochum, 2019.

[17] L. Merten et al. In: *The Astroph. J.* 859, 63 (2018).

[18] S. Miyake et al. In: *Astron. & Astroph.* 573, A134 (Jan. 2015).

[19] A. Shalchi. Astrophysics and Space Science Library. Springer Berlin Heidelberg, 2009. ISBN: 9783642003097.

[20] A. Strong and I. Moskalenko. In: *The Astroph. J.* 509 (Dec. 1998).

[21] S. Thoudam et al. In: *Astron. & Astroph.* 595, A33 (2016).

[22] V. I. Zatsepin and N. V. Sokolskaya. In: *Astron. & Astroph.* 458 (2006).